Supporting Information

Peyrache et al. 10.1073/pnas.1109895109

SI Materials and Methods

Unit Recording and Spike Sorting. For offline sorting, the first three principal components of spike waveforms were computed independently for recordings from each electrode. The spikes were then clustered automatically with an expectation–maximization (E-M) algorithm (Klustakwik, http://klustakwik.sourceforge.net) and then manually processed with Klusters software (http://klusters.sourceforge.net/). Because the signal was sometimes not stable, great care was taken during spike cluster cutting. Some cells with drifting action potential amplitudes were considered only for a portion of the total recording during which they were unequivocally distinguishable from the background noise. In that case, the average firing rates were computed only over the period those cells were firing.

Discrimination of Pyramidal (Pyr) Cells and Fast-Spiking (FS) Interneurons (Int). Average waveforms were computed for each isolated cell. As described previously, the half width of the extracellular positive deflection has, at the neuronal population level, a bimodal distribution (1, 2). The separation is even more striking when the valley-to-peak parameter (2) is added for 2D clustering (Fig. 2 *A* and *B*). Automatic clustering of these average waveforms from individual cells by using a *k*-means algorithm discriminated two groups of cells (Fig. 2 *A* and *B*). The resultant clustering was further confirmed by an E-M clustering method (Fig. S1).

Detecting Monosynaptic Connections from Cross-Correlograms. We used established methods (3) to detect statistically significant temporal bias in the cell pair relative spike timing indicative of putative monosynaptic connections. The spikes were jittered by adding a random value (from a normal distribution with a 10-ms SD and 0 mean) to the spike times. For each cell pair, 1,000 jittered spike trains were created, and the expected cross-correlogram (and 99% confidence interval) was estimated on 0.5-ms time bins under the null hypothesis of no monosynaptic effects between the two cells. For any given cell pair where at least two consecutive bins in the [1.5 ms, 4 ms] interval exceeded or were below the 99% confidence interval, the interaction was considered monosynaptic. A final and blind examination of the cell pair cross-correlograms was carried out to remove noisy pairs. The strength of the interaction was defined, at the time lag of maximal (or minimal) value in the actual cross-correlogram, as the ratio between the value of the actual cross-correlogram (from which was subtracted the average value expected for uncorrelated units) and the SD of the distribution from jittered spike trains.

Nonstationary Correlation. The firing rates of neurons may not be stationary over the long recordings performed in the present study. To avoid any potential bias that could result from such long-timescale fluctuations, we filtered the spike trains so that only local firing rates were taken into account (4). The binned spike trains (in time bins of the indicated length) were filtered with a "Mexican hat"-shaped kernel, equal to the sum of a positive (width T) and a negative Gaussian function whose width is the quadratic mean of T and a value J. Throughout the present paper, we used $T = 3$ (expressed in number of time bins) and $J = 4T$. The covariance between two neurons' firing was obtained by computing the dot product of the resulting filtered and binned spike trains. The correlation was calculated by dividing the covariance by the product of the square roots of the two individual variances (the dot product of the filtered binned spike train with itself). Only cells with an average firing rate above 0.1 Hz were included in the correlation study unless stated otherwise.

Sleep Scoring. The postimplantation recordings were performed during clinical monitoring for seizures. We used a combination of video monitoring, scalp EEG, electrooculography (EOG), and clinical intracranial EEG to stage the sleep. The sleep staging was carried out in three of the four recording sessions (comprising 87% of the neural data). Rapid eye movement (REM) episodes were too brief; therefore, we did not include REM in our analysis. Nonetheless, all states—including clear episodes of quiet waking/drowsiness, light non-rapid eye movement (NREM), and deep NREM—were present during all recordings. In this paper, we focused on these states and excluded the rare REM episodes as well as periods when the patient was interacting with medical personnel. In addition, any seizure activity (one event in one patient) was removed from the data and not further analyzed.

Electrode Localization. The electrode-localization procedure was based on combining coregistration of high-resolution preoperative MRI with postoperative computed tomography (taking into account the parenchymal shift introduced by the implantation) and 3D rendering of each patient's cortical surface [these methods are described by Dykstra et al. (5)].

1. McCormick DA, Connors BW, Lighthall JW, Prince DA (1985) Comparative electrophysiology of pyramidal and sparsely spiny stellate neurons of the neocortex. *J Neurophysiol* 54:782–806.
2. Barthó P, et al. (2004) Characterization of neocortical principal cells and interneurons by network interactions and extracellular features. *J Neurophysiol* 92:600–608.
3. Fujisawa S, Amarasingham A, Harrison MT, Buzsáki G (2008) Behavior-dependent short-term assembly dynamics in the medial prefrontal cortex. *Nat Neurosci* 11:823–833.
4. Renart A, et al. (2010) The asynchronous state in cortical circuits. *Science* 327:587–590.
5. Dykstra et al. (2011) Individualized localization and cortical surface-based registration of intracranial electrodes. *Neuroimage*, 10.1016/j.neuroimage.2011.11.046.

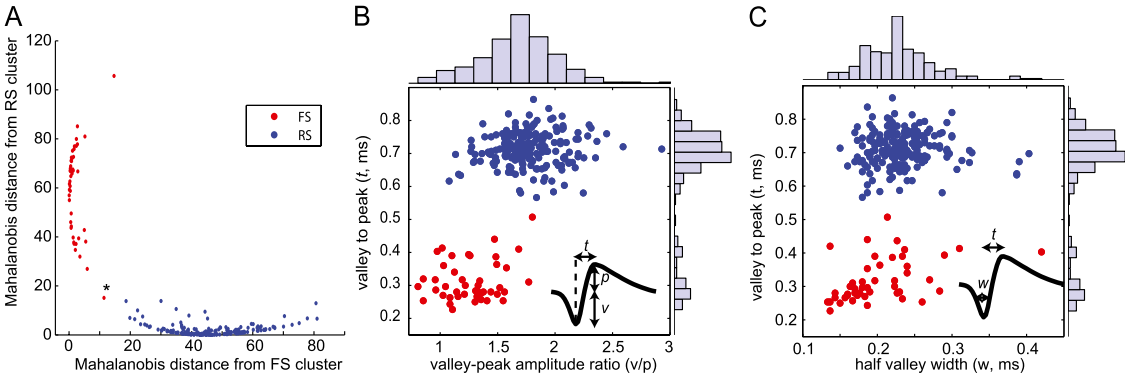

Fig. S1. Separation of regular-spiking (RS) and FS cells with a Gaussian mixture model. The E-M algorithm was used to obtain maximum likelihood estimates of the parameters in a Gaussian mixture model with two components for an *n*-by-*d* data matrix, where $n = 238$ is the number of observations (individual cells pooled together from all subjects) and $d = 2$ is the dimension of the data (valley-to-peak and half-peak widths). The Mahalanobis distance (in squared units) of each observation to the mean of each of the two components of the Gaussian mixture distribution (described above) was computed. The plotted results form a curve in a non-Euclidean space where those above the diagonal represent FS and those below show RS characteristics. The asterisk indicates the only mismatching point between the two clustering procedures. (*B*) Spike waveform clustering using valley-to-peak amplitude ratio and valley-to-peak widths. Colors indicate clustering based on the features used in the main text (half-peak width and valley-to-peak distance). (*C*) Same as in *B* but using half-valley width and valley-to-peak distance.

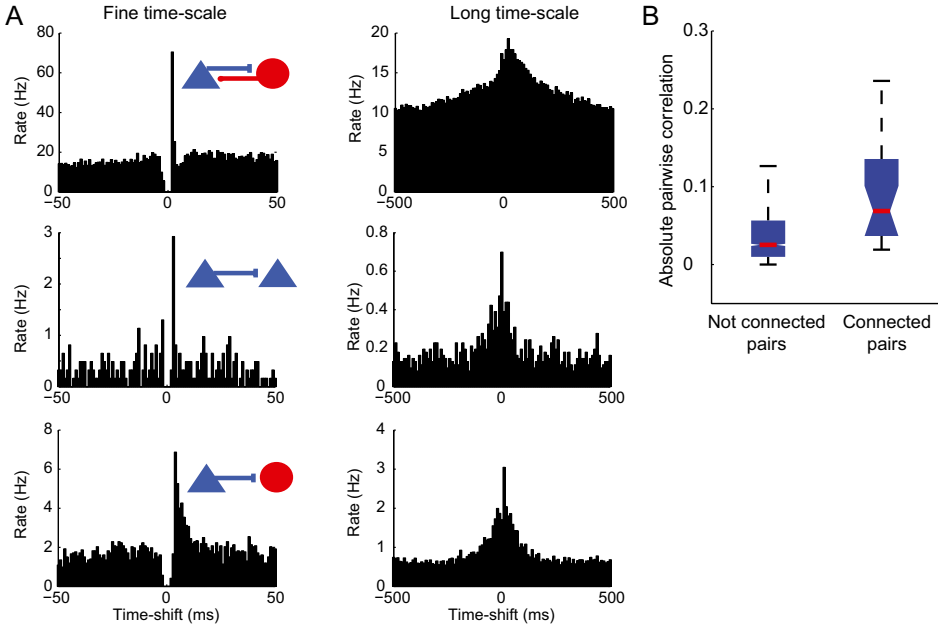

Fig. S2. Correlation between pairs recorded on the same electrodes depended on their connectivity. (*A*) Examples of putative monosynaptically connected cells as revealed by the short-timescale cross-correlograms. At a longer timescale, the cross-correlograms tended to show positive peaks indicative of strong correlation. (*B*) Box plot of absolute correlation of binned spike trains (using 50-ms bins) depicting interquartile distribution. Correlations were significantly stronger for monosynaptically connected pairs ($P < 0.0001$, one-way ANOVA).

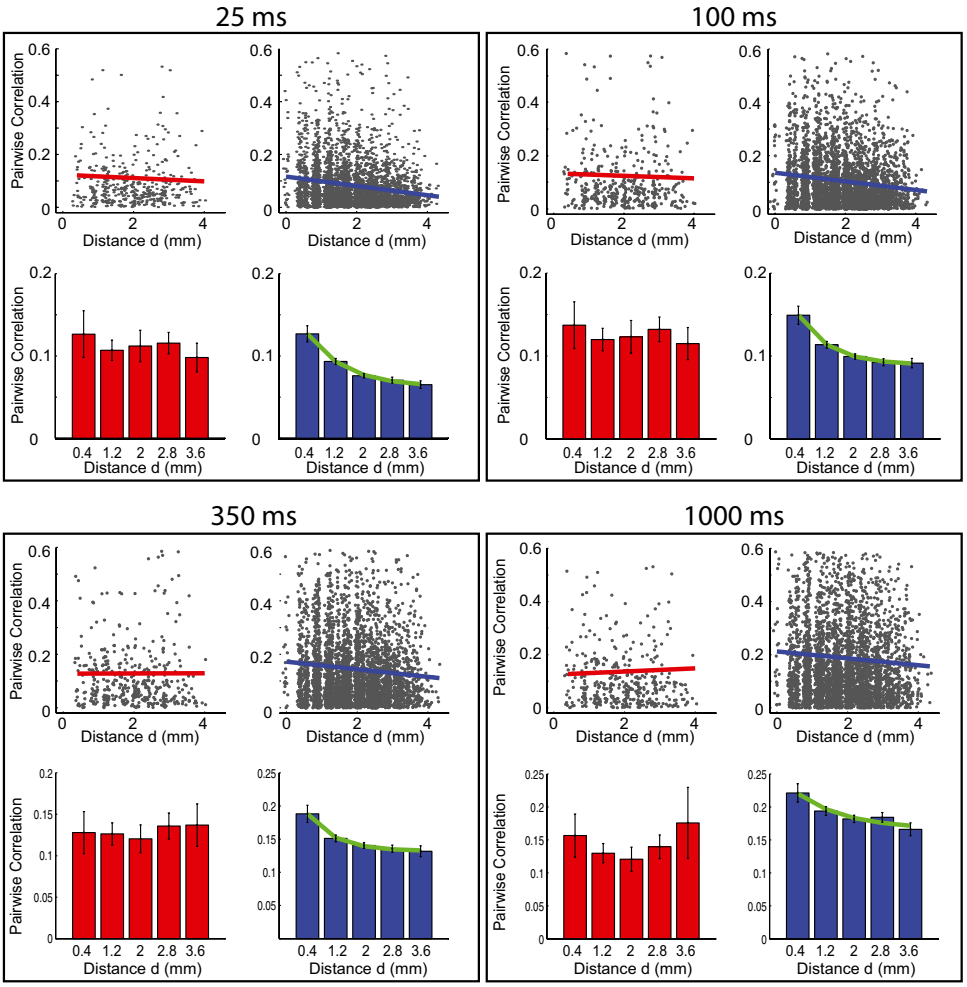

Fig. S3. Correlations calculated for different time bins. The same plots are shown as in Fig. 5 *A* and *C* but for different time bins.

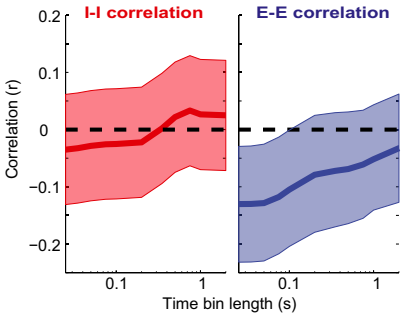

Fig. S4. Same analysis as in Fig. 5B, correlation between neuronal pairwise correlations and relative distance. Here, the number of RS cell pairs (E–E, blue) was down-sampled so that it matched the number of FS cell pairs (I–I, red). Shaded areas of the E–E spatial correlation indicate the 95% confidence interval obtained by bootstrapping the down-sampled pairs (5,000 random samplings).

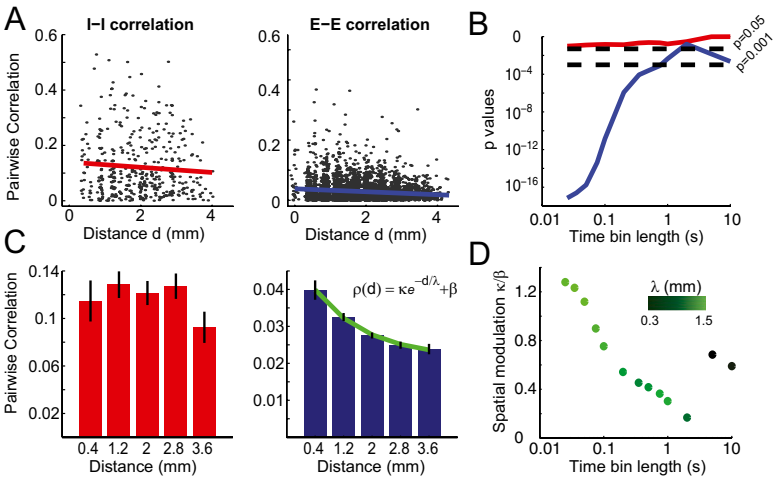

Fig. S5. Same as in Fig. 5 but with nonnormalized coefficients of correlation. In this case, correlation values were no longer comparable between the two groups of neurons. *B* shows the *P* values of linear regression.